Cyclic deformation behavior and intergranular fatigue cracking of a copper bicrystal with a parallel grain boundary

Z.F. Zhang *, Z.G. Wang, Y.M. Hu

Chinese Academy of Sciences, State Key Laboratory for Fatigue and Fracture of Materials, Institute of Metal Research, 72 Wenhua Road, Shenyang, 110015, PR China

Abstract

Cyclic deformation behavior and intergranular fatigue cracking of a $[\bar{4}\ 9\ 16]/[\bar{4}\ 9\ 27]$ copper bicrystal with a grain boundary (GB) parallel to the stress axis were investigated under constant plastic strain control at room temperature in air. It was found that cyclic saturation stresses of the bicrystal increased with increasing strain amplitude, and were higher than the plateau stress of 28–30 MPa, if modified by an orientation factor Ω_B of the bicrystal. Surface observations showed that a GB affected zone (GBAZ) with secondary slip formed owing to plastic strain incompatibility near the GB. As cyclic deformation was continued, fatigue cracks always initiated at the intersection sites of persistent slip bands (PSBs) with the GB. Gradually, they linked each other along the GB, leading to intergranular cracking. However, fatigue crack nucleating along slip bands was not observed as intergranular cracking occurred. It is indicated that intergranular fatigue cracking is the major damage mode even though the GB was parallel to the stress axis. Based on the results above, the GB strengthening effect and intergranular fatigue cracking mechanism were discussed in combination with the GBAZ and the interaction between PSBs and GB. © 1999 Elsevier Science S.A. All rights reserved.

Keywords: Copper bicrystal; Cyclic deformation; GB affected zone; GB strengthening; Intergranular fatigue cracking

1. Introduction

It is well-known that copper single crystals oriented for single slip exhibited a plateau region over a wide resolved shear plastic strain range from 6.0×10^{-5} to 7.5×10^{-3} in its cyclic stress–strain (CSS) curve [1,2]. Cheng and Laird [3] found that the plateau saturation resolved shear stress at room temperature was in the range of 28–30 MPa, which represented the critical stress needed to activate persistent slip bands (PSBs). Meanwhile, cyclic deformation behavior of copper polycrystals was widely investigated. Some investigators found that the CSS curves of copper polycrystals with different grain sizes also exhibited a plateau feature over a certain strain range [4–7]. However, Mughrabi [8], Lukas and Kunz [9] urged that there should be no apparent plateau in the CSS curve of copper polycrys-

tals. Essentially, there are two important factors affecting the cyclic deformation behavior of polycrystals, i.e. crystal orientation and grain boundary (GB). All the grains oriented randomly and the GBs often lead to elastic and plastic strain incompatibility. To clarify the difference in fatigue behavior between monocrystals and polycrystals, a bicrystal can be regarded as an ideal model material. Firstly, a $[\bar{4}\ 9\ 16]/[\bar{4}\ 9\ 27]$ copper bicrystal with a GB parallel to the stress axis was selected to further investigate the GB effect on cyclic stress–strain response and surface slip morphology.

On the other hand, fatigue crack nucleation plays a substantial role in fatigue failure of materials. For monocrystalline materials, a fatigue crack is often developed from the surface roughness caused by the interaction of the surface with PSBs [10–15], whereas, for pure polycrystalline materials, numerous experimental observations revealed that both the GBs [16–24] and the interface of PSBs with the matrix can become the preferential sites to initiate fatigue cracks. Kim and Laird [23,24] have developed a step-mechanism for

---

* Corresponding author. Tel.: + 86-24-23843531; fax: + 86-24-23891320.

E-mail address: zhfzhangf@imr.ac.cn (Z.F. Zhang).

intergranular fatigue cracking in polycrystalline copper fatigued at high strain amplitudes. One of the conditions for this step-mechanism is that the interaction angles of the stress axis with the GB should be in the range of 30–90°. It means that the step-mechanism for intergranular cracking may be invalid as the GB is parallel to the stress axis. Recently, it has been observed that fatigue cracks always initiated and propagated along GB in the copper bicrystals with a perpendicular GB during cyclic deformation [25–29]. However, it is very ambiguous whether the GB will become the site to initiate fatigue cracks in those bicrystals with a parallel GB [30–32]. In our previous work [33,34], the cyclic stress–strain responses of [$\bar{1}$35]/[$\bar{1}$35], [$\bar{1}$35]/[$\bar{2}$35], [$\bar{2}$35]/[$\bar{2}$35] and [$\bar{6}$79]/[$\bar{1}$45] copper bicrystals with a parallel GB were systematically investigated. Unfortunately, fatigue cracking behavior in those bicrystals was not studied. In this paper, focus will be placed on the fatigue cracking mechanism in a [$\bar{4}$ 9 16]/[$\bar{4}$ 9 27] copper bicrystal.

2. Experimental procedure

A bicrystal with the size of $60 \times 20 \times 10$ mm^3 was grown from OFHC copper of 99.999% purity by the Bridgman method. Two fatigue specimens with a parallel GB were made from the bicrystal plate. By electron back-scatter diffraction (EBSD) technique, the orientations of the two component crystals in the bicrystal were determined as follows

$$G1 = \begin{bmatrix} RD & TD & ND \\ 0.5929 & 0.2148 & 0.7761 \\ -0.2988 & -0.8362 & 0.4598 \\ 0.7478 & -0.5045 & -0.4316 \end{bmatrix} \text{ and } G2 = \begin{bmatrix} RD & TD & ND \\ 0.7205 & -0.3056 & -0.6224 \\ 0.6134 & -0.1376 & 0.7777 \\ 0.3233 & 0.9422 & -0.0884 \end{bmatrix}$$

In brief, the crystallography of each grain of the bicrystal can be given as

$$G1 = \begin{bmatrix} RD & TD & ND \\ 4 & 4 & 7 \\ -2 & -16 & 4 \\ 5 & -9 & -4 \end{bmatrix} \text{ and } G2 = \begin{bmatrix} RD & TD & ND \\ 22 & -9 & -7 \\ 19 & -4 & 9 \\ 10 & 27 & -1 \end{bmatrix}$$

Herein, TD represents the stress axis orientations of component crystals, and the bicrystal can be denoted as [$\bar{4}$ 9 16]/[$\bar{4}$ 9 27]. Fig. 1a gives the stress axis orientations of two crystals in the stereographic triangle, clearly, both crystals G1 and G2 are oriented for single slip. Fig. 1b shows the crystallographic relations between primary slip plane and the GB along with the size of the specimen gauge. It is apparent that the primary slip planes of two component crystals are not coplanar. Before cyclic deformation, the two bicrystal specimens were electro-polished carefully for surface observation. Cyclic push-pull tests were performed on a Shimadzu

servo-hydraulic testing machine under constant plastic strain control at room temperature in air. A triangle wave with a frequency range of 0.1–0.5 Hz was used. The peak loads in tension and compression were recorded continuously and the hysteresis loops were registered in intervals on an X-Y recorder until cyclic saturation occurred. The applied axial plastic strain amplitudes ($\Delta\varepsilon_{pl}/2$) are equal to 5×10^{-4} and 2.0×10^{-3}, respectively (denoted as bicrystal B-50 and B-200). After cyclic saturation, the slip morphology on the bicrystal surfaces were observed by scanning electron microscopy (SEM). Afterwards, cyclic deformation was continued and interrupted at different cycles to examine fatigue cracks by SEM.

3. Experimental results

3.1. Cyclic hardening and saturation behavior

During cyclic deformation, the two bicrystals exhibited rapid cyclic hardening and saturation behavior with axial saturation stresses of 67 MPa (B-50, $\varepsilon_{pl} = 5 \times 10^{-4}$) and 71 MPa (B-200, $\varepsilon_{pl} = 2 \times 10^{-3}$), respectively. The cyclic hardening curves are shown in Fig. 2. It can be seen that the initial hardening rate of the bicrystal B-200 was distinctly higher than that of the bicrystal B-50. It means that hardening rate of the present bicrystal increased with increasing strain amplitude, similar to that of single-slip copper single crystals [1]. In addition, the saturation stresses of bicrystals B-50 and B-200 are not the same even though the orientations of two component crystals in the two bicrystals are identical and oriented for single-slip. It is indicated that the saturation stress of the bicrystal also increased with increasing strain amplitude, which is quite different from that in copper single crystals with single-slip orientations. Accordingly, it is suggested that the cyclic stress–strain (CSS) curve of the bicrystal should not display an apparent plateau feature, similar to that of [$\bar{6}$79]/[$\bar{1}$45] copper bicrystal [34]. This may be
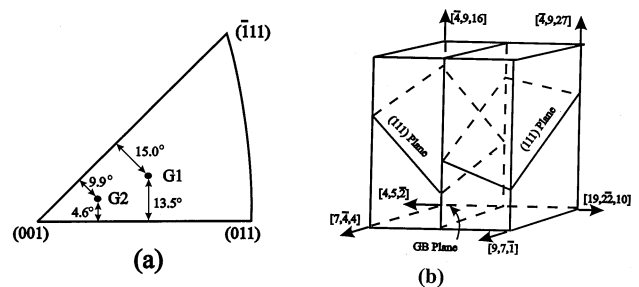

Fig. 1. Fatigue specimen and crystallographic relation of a [$\bar{4}$ 9 16]/[$\bar{4}$ 9 27] copper bicrystal. (a) Axis orientations of component grain in the stereographic triangle; (b) crystallography of two component crystals in the bicrystal.
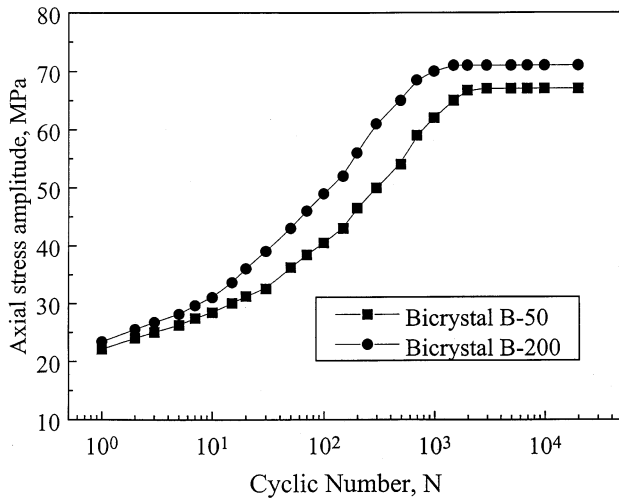
Fig. 2. Cyclic hardening curves of the bicrystals B-50 ($\varepsilon_{pl} = 5 \times 10^{-4}$) and B-200 ($\varepsilon_{pl} = 2 \times 10^{-3}$).

attributed to the GB strengthening effect and will be discussed in a later section.

3.2. Surface slip morphology

By SEM, the surface slip morphologies of the bicrystals B-50 and B-200 were observed. It was found that, on the crystal G1[$\bar{4}$ 9 16] surface for both bicrystals B-50 and B-200, only the primary slip bands (B4) were activated. However, on the crystal G2[$\bar{4}$ 9 27] surface, the slip morphology in the bicrystal B-200 are not the same as that in the bicrystal B-50 owing to the difference in applied strain amplitude. Fig. 3a shows the surface slip morphology of the bicrystal B-50, it can be seen that the primary slip bands within crystal G2 cannot reach the GB, but were terminated at certain distance from the GB. In the vicinity of the GB, there formed a GB affected zone (GBAZ) only containing secondary slip bands (A3). The width of the GBAZ within the crystal G2 was about 500–600 μm in the bicrystal B-50. Fig. 3b demonstrates the slip morphology of the bicrystal B-200, in this case, all the primary slip bands within the crystals G1 and G2 can reach the GB. Similar to the bicrystal B-50, there is also a GBAZ, in the bicrystal B-200. However, the width of the GBAZ and the total number of activated slip systems within the GBAZ in the bicrystal B-200 are obviously different from those in the bicrystal B-50. Wherein, both the primary (B4) and secondary slip bands (A3) appeared near the GB, forming a GBAZ with weaved structure in the bicrystal B-200, as shown in Fig. 3c. In particular, the bicrystal B-200 displayed much more serious plastic strain incompatibility and the width of GBAZ was enlarged to 800–1000 μm. The difference above should be attributed to the increase in applied strain amplitude.

In addition, it was noted that the GBAZ only appeared within crystal G2 for the two bicrystals during cyclic deformation. Meanwhile, the relatively high Schmid factors of each grain in the bicrystal were calculated and listed in Table 1. First, it can be seen that the Schmid factor of slip system A3 of grain [$\bar{4}$ 9 27] is equal to 0.455, and higher those (0.402, 0.318) of slip systems (A3 and C1) of grain [$\bar{4}$ 9 16] as well as that (0.391) of slip system C1 of grain [$\bar{4}$ 9 27]. Second, as shown in Fig. 1a, the angles of [$\bar{4}$ 9 27] orientation with double slip [0 9 2 7] and [$\bar{9}$ 9 27] orientations are equal to 4.6 and 9.9°, respectively. In particular, the [0 9 27]
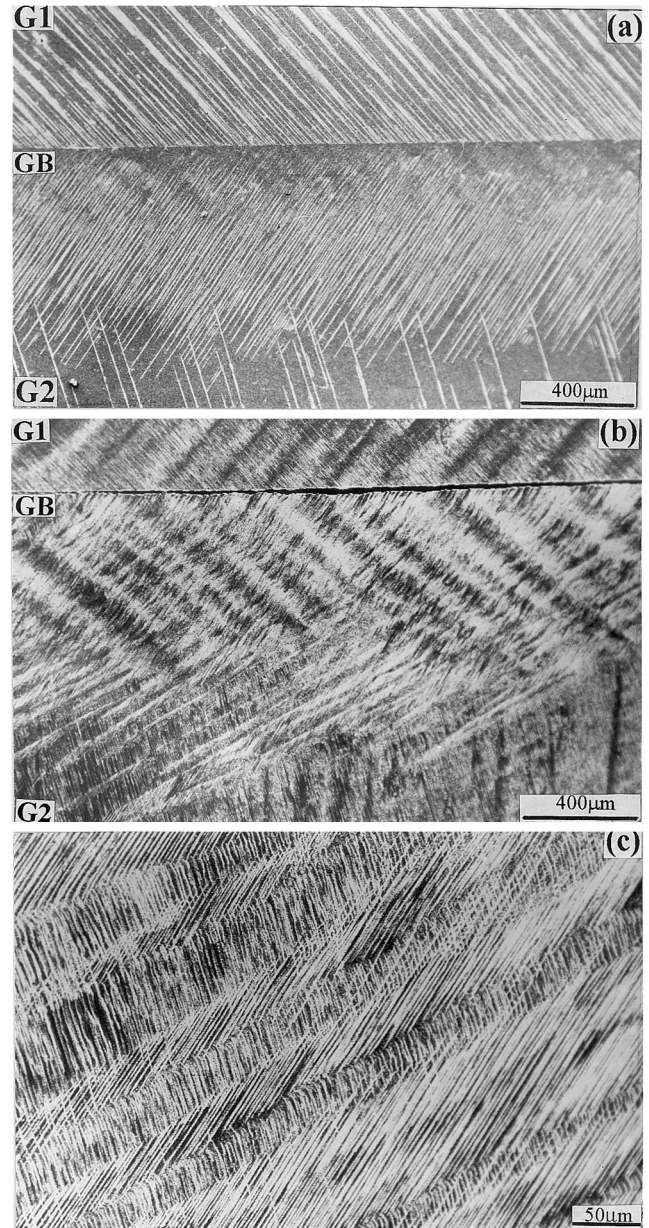

Fig. 3. Surface slip morphology of the bicrystals B-50 and B-200. (a) Bicrystal (B-50) deformed at $\varepsilon_{pl} = 5 \times 10^{-4}$; (b) bicrystal (B-200) deformed at $\varepsilon_{pl} = 2 \times 10^{-3}$; (c) slip morphology within the GB affected zone (GBAZ) in the bicrystal B-200.

Table 1
Relatively high Schmid factors of each grain in the bicrystal

	B4	A3	C1
[$\bar{4}$ 9 16] grain	0.486	0.402	0.318
[$\bar{4}$ 9 27] grain	0.490	0.455	0.391

is typical conjugate orientation (B4 and A3). Whereas, the angles of [$\bar{4}$ 9 16] orientation with double slip [0 9 16] and [$\bar{9}$ 9 16] orientations are equal to 13.5 and 15°, respectively. It means that the crystal G2[$\bar{4}$ 9 27] is more close to the double-slip orientation than the crystal G2[$\bar{4}$ 9 16]. Accordingly, the operation of secondary slip system (A3) of crystal G2 [$\bar{4}$ 9 27] should be easier than those of the crystal G1[$\bar{4}$ 9 16] under the strain of the GB.

Recently, Zhang and Wang [34] found that the number of the activated slip systems near the GB in a [$\bar{6}$79]/[$\bar{1}$45] copper bicrystal was always equal to three at the plastic strain range of 3.3×10^{-4} to 2.3×10^{-3}. If taking the criticism of Kocks [35] into account, the total number of activated slip systems beside a GB should be equal to four. However, in [$\bar{6}$79]/[$\bar{1}$45] and the present copper bicrystals, the total number of activated slip systems near the GB are only equal to two or three, respectively. Apparently, the result is not consistent with the conclusion by Kocks. It is suggested that the total number of activated slip systems next to a GB strongly depends on the orientations of component crystals and applied strain amplitude, and might not be a constant of four for the bicrystals subjected to cyclic deformation.

3.3. Fatigue cracking behavior

By SEM, the surfaces of the two bicrystals were observed at different cycles to examine fatigue cracks. It was found that all the fatigue cracks nucleated along the GB in both bicrystals B-50 and B-200 after cyclic saturation. For the bicrystal B-50, it was rather difficult to initiate intergranular cracks. As the cycle was increased to about 5×10^4, the fatigue crack was not quite clear, as shown in Fig. 4a. With continuing to cyclically deform, fatigue cracks began to be distinguished, as shown in Fig. 4b. Step by step, those fatigue cracks propagated and linked each other along the GB (see Fig. 4c). For the bicrystal B-200, initiating fatigue cracks was very easy since the applied strain amplitude was relatively high. Fig. 5a shows the fatigue cracks in the bicrystal B-200 after 10^4 cycles. It can be seen that fatigue cracks always nucleated along the GB rather than along the slip bands even though strong secondary slip appeared in the GBAZ. As cycling was continued, those cracks also propagated and linked along the GB, as shown in Fig. 5b. Gradually, the crack penetrated

through the whole GB, forming a rift with a width of about 10 μm (see Fig. 5c). It is apparent that all the fatigue cracks preferentially nucleated at the intersection sites of PSBs with the GB, then propagated and linked along GB, leading to intergranular cracking. Those observations should support a powerful evidence for the PSB-GB damage mechanism [10,19,20,22]. Meanwhile, the component crystal surfaces were also observed to examine whether fatigue crack can nucleate along surface slip bands. The result showed that there was no any crack initiating along surface slip bands until intergranular cracks initiated. It is indicated that intergranular cracking is the dominant fatigue damage mode in the [$\bar{4}$ 9 16]/[$\bar{4}$ 9 27] bicrystal with a parallel GB
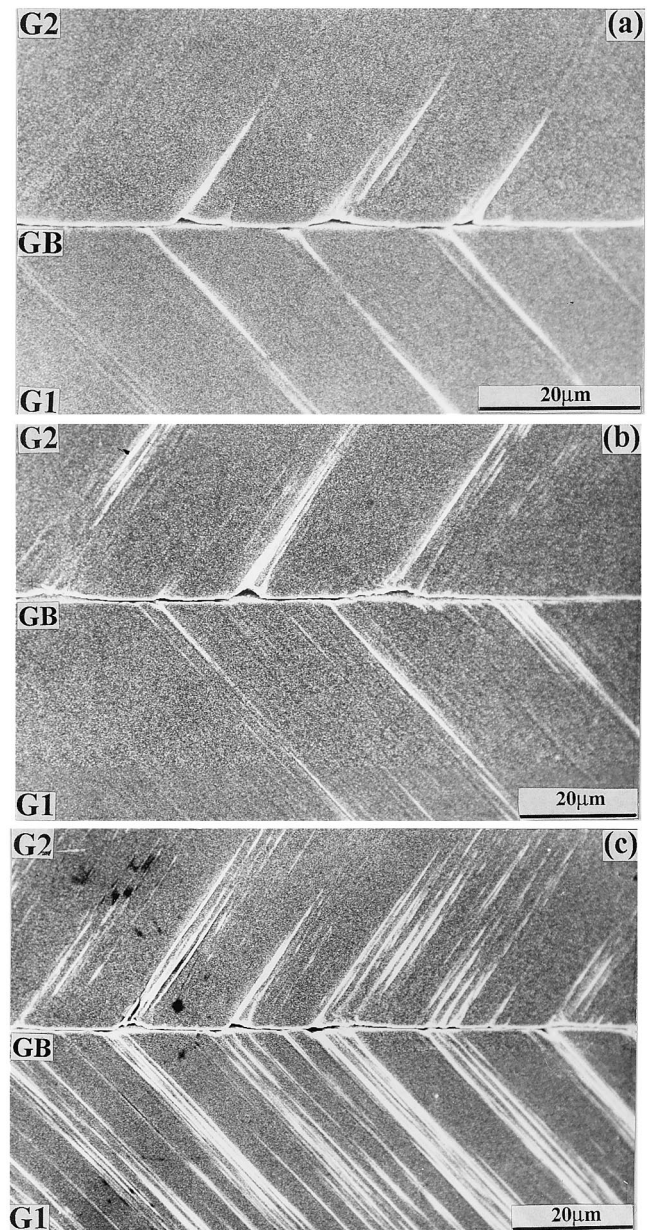

Fig. 4. Intergranular fatigue cracking in the bicrystal B-50 deformed at $\varepsilon_{pl} = 5 \times 10^{-4}$. (a) $N = 2 \times 10^4$; (b) $N = 5 \times 10^4$; (c) $N = 2 \times 10^5$.
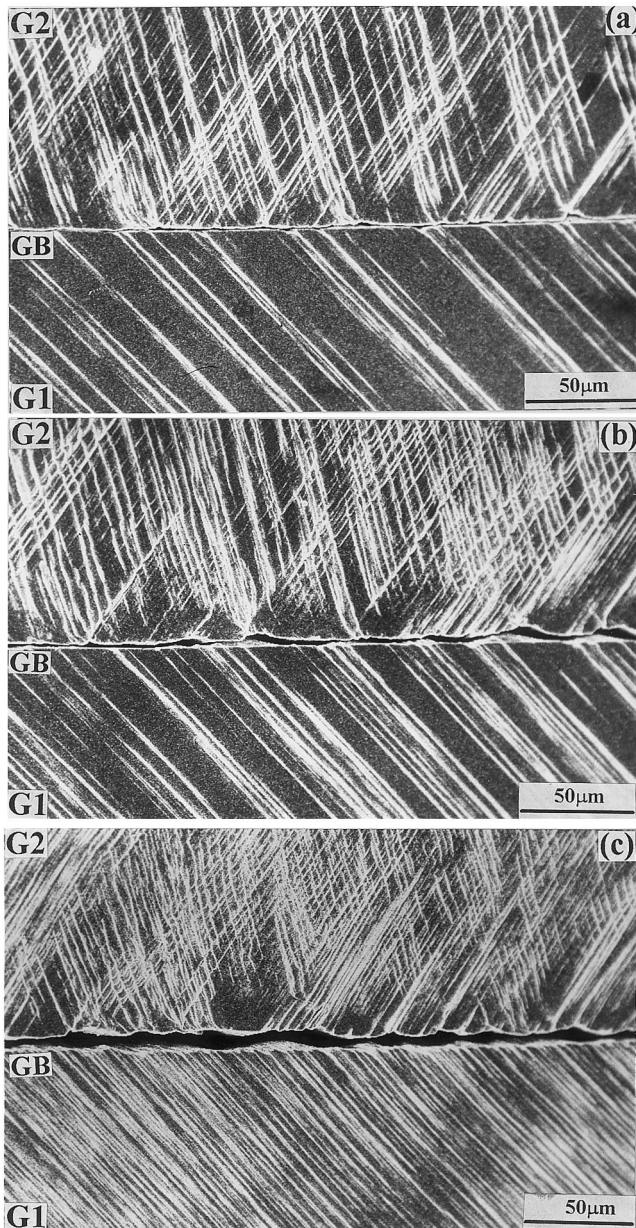
Fig. 5. Intergranular fatigue cracking in the bicrystal B-200 deformed at $\varepsilon_{pl} = 2 \times 10^{-3}$. (a) $N = 10^4$; (b) $N = 2 \times 10^4$; (c) $N = 5 \times 10^4$.

as well as those copper bicrystals containing a perpendicular GB [25–29]. In other words, intergranular fatigue cracking can take place in the bicrystals with not only a perpendicular GB, but also a parallel GB.

4. Discussion

4.1. Grain boundary strengthening effect

According to Cheng and Laird's conclusion [3], if a copper single crystal with single-slip orientation is cyclically deformed at the plastic strain range of plateau region, its axial saturation stress σ_{as}^{G} will be equal to

$$\sigma_{as}^{G} = \tau_{as}^{PSB}/\Omega \tag{1}$$

where, τ_{as}^{PSB} is the stress activating PSBs and equal to 28–30 MPa, Ω is the Schmid factor of the primary slip system of the single crystal. Similarly, for a copper bicrystal with two single-slip-oriented component crystals and a parallel GB, if regardless of the GB effect, as shown in Fig. 6a and b, its axial saturation stress σ_{as}^{B} should be equal to

$$\begin{aligned} \sigma_{as}^{B} &= \sigma_{as}^{G1}V_{G1} + \sigma_{as}^{G2}V_{G2} \\ &= V_{G1}\tau_{as}^{PSB}/\Omega_{G1} + V_{G2}\tau_{as}^{PSB}/\Omega_{G2} \\ &= \tau_{as}^{PSB}(V_{G1}/\Omega_{G1} + V_{G2}/\Omega_{G2}) \end{aligned} \tag{2}$$

where, V_{G1} and V_{G2} are the volume fractions of the crystals G1 and G2 in the bicrystal, Ω_{G1} and Ω_{G2} are the Schmid factors of the primary slip systems of the crystals G1 and G2 and equal to 0.486 and 0.490, respectively. Submitting $V_{G1} = V_{G2} = 0.5$, $\tau_{as}^{PSB} = 28$–30 MPa, $\Omega_{G1} = 0.486$ and $\Omega_{G2} = 0.490$ into Eq. (2), the axial saturation stress of the bicrystal should be in the range of 57.3–61.4 MPa. Obviously, the calculated axial saturation stress by Eq. (2) is smaller than the experimental value of 67 and 71 MPa, which should be attributed to the strengthening effect of the GB or the GBAZ.

By surface observations, it has been found that strong interaction of PSBs with GB can lead to the formation of a GBAZ. In turn, the GB or GBAZ would affect the cyclic stress–strain response of the bicrystal. Previously, GB strengthening effect on copper and β-brass bicrystals had been observed and explained by Rey and Zaoui [36,37], Margolin et al. [38–40]. In our recent work [33,34], it was also observed that the saturation stresses of $[\bar{1}35]/[\bar{1}35]$, $[\bar{1}35]/[\bar{2}35]$, $[\bar{2}35]/[\bar{2}35]$ and $[\bar{6}79]/[\bar{1}45]$ copper bicrystals were obviously higher than that of single crystals owing the presence of the GB. Similarly, the saturation stress of the $[\bar{4}\ 9\ 16]/[\bar{4}\ 9\ 27]$ bicrystal can be expressed as follows
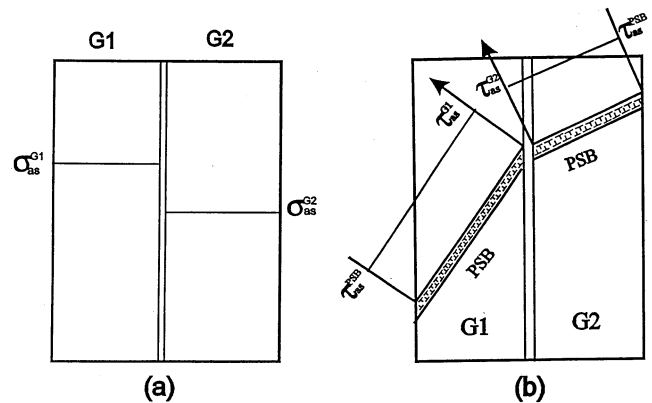

Fig. 6. Schematic sketches of stress distribution in the bicrystal, wherein, the effect of the GB is not considered. (a) Axial stress distribution; (b) resolved shear stress distribution.
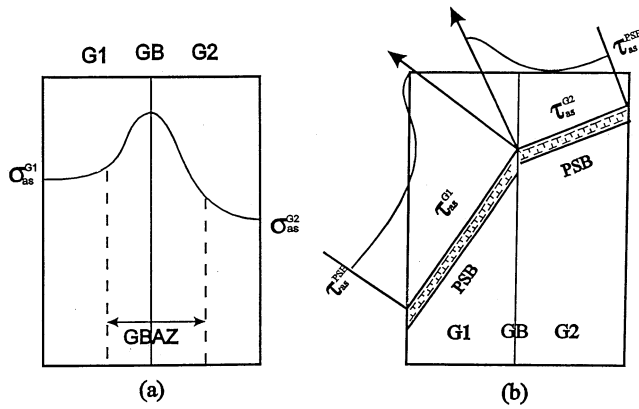
Fig. 7. Schematic sketches of stress distribution in the bicrystal, herein, the effect of the GB is considered. (a) Axial stress distribution; (b) resolved shear stress distribution.

$$\sigma_{as}^{B} = \sigma_{as}^{G1} V_{G1} + \sigma_{as}^{G2} V_{G2} + \sigma_{as}^{GB} \qquad (3)$$

where, σ_{as}^{GB} can be defined as the stress increase caused by the GB or GBAZ, and should be in the range of 5.6–9.7 and 9.6–13.7 MPa, respectively for bicrystals B-50 and B-200. If introducing an orientation factor Ω_{GB} of bicrystal [34]

$$\Omega_{B} = (V_{G1}/\Omega_{G1} + V_{G2}/\Omega_{G2})^{-1} \qquad (4)$$

the saturation resolved shear stress of the bicrystal will be calculated as

$$\tau_{as}^{B} = \sigma_{as}^{B}\Omega_{B} = \sigma_{as}^{B}(V_{G1}/\Omega_{G1} + V_{G2}/\Omega_{G2})^{-1} \qquad (5)$$

By Eq. (5), the calculated saturation resolved shear stress of the bicrystals B-50 and B-200 are equal to 32.7 and 34.7 MPa. Clearly, the stress values (32.7 and 34.7 MPa) of the two bicrystals are distinctly higher than 28–30 MPa of single-slip oriented crystals. The increase in saturation stress of the bicrystals can be explained as the resistance of GB to PSBs. The sketch of GB strengthening effect on the bicrystals can be illustrated in Fig. 7a and b. Meanwhile, noted that the GBAZ was enlarged and displayed more serious plastic strain incompatibility with increasing strain amplitude (see Fig. 3a–c). As a result, the saturation stress of the bicrystal B-200 was obviously higher than that of the bicrystal B-50, which is in good agreement with that of [$\bar{6}$79]/[$\bar{1}$45] copper bicrystal [34]. The GB strengthening effect on copper bicrystals will provide a fundamental understanding on the CSS curves of copper polycrystals [1–9].

4.2. Intergranular fatigue cracking mechanism

For pure f.c.c. single crystals, it was observed that fatigue crack initiation is always associated with the formation of PSBs, which carried out most of plastic strain during cyclic deformation. The observations on fatigue crack initiation along PSBs in copper single crystals are elsewhere, for example, by Essmann et al. [10], Basinski and Basinski [12], Laird et al. [11,14], Husche and Neumann [13]. The PSB damage mechanism during cyclic deformation was often explained as the surface roughness caused by slip irreversibility by Essmann et al. [10] and was simulated by Repetto and Ortiz [15]. However, for a ductile bicrystal containing a large-angle GB, the study on fatigue cracking behavior is very limited. In recent study [25–29], it was observed that intergranular crack initiation and propagation were rather easy in those copper bicrystals with a perpendicular GB after cyclic deformation. Kim and Laird [23,24] had proposed a step mechanism for intergranular cracking in copper polycrystals fatigued at higher strain amplitude. It is noted that the interaction angles of GB with the stress axis must be in the range of 30–90° for the step-mechanism. It means that this mechanism cannot be applied to the fatigue cracking of those bicrystals with a parallel GB. Afterwards, Essmann et al. [10] attributed the intergranular cracking to the piling-up of PSBs at GB, and defined this process as PSB-GB damage mechanism. Liu et al. [19] discussed the relationship between intergranular cracking and the interactions of PSBs with GBs in fatigued copper polycrystals using the EBSD technique. However, it is not very clear what kinds of role the GB will play in intergranular cracking, especially, as the GB is parallel to the stress axis. From the results above, the PSB-GB mechanism can also be used to explain the intergranular fatigue cracking of the present bicrystals and will be discussed as follows.

It has been well known that most of plastic strains are carried by PSBs and mounts of defects (including dislocations and vacancies) are produced during cyclic plastic deformation of metallic materials. PSB may become a carrier or channel transporting residual dislocations (or vacancies) from interior of grains into GBs according to the PSB-GB cracking mechanism. Therefore, the interaction of PSBs with the GB in bicrystal B-50 can be simply illustrated in Fig. 8a, in which the primary slip bands within crystal G2 can not reach the GB during cyclic deformation (see Fig. 3a). Apparently, those residual dislocations carried by PSBs will be
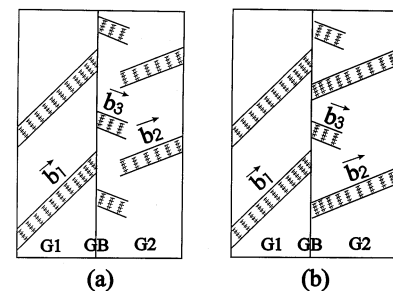

Fig. 8. Interactions of PSBs with the GB in the two bicrystals. (a) Bicrystal B-50; (b) bicrystal B-200.

piled-up at the GB and cannot pass through. Meanwhile, the secondary slip bands within the crystal G2 can also transport some residual dislocations into the GB. If the Burgers vectors of residual dislocations carried by those PSBs from crystals G1 and G2 into the GB are b_1 and b_3, respectively, the Burgers vector sum b_{GB} of residual dislocations piled-up at the GB in bicrystal B-50 can be expressed as

$$b_{GB} = b_1 - b_3 \qquad (6)$$

Obviously, b_1 is not equal to b_3 owing to the large disorientation between crystals G1 and G2. This can also be proved by the surface slip morphology in Figs 3a and 4. Thus, the Burgers vector sum b_{GB} of residual dislocations piled-up at the GB in bicrystal B-50 was not equal to 0, i.e.

$$b_{GB} \neq 0 \qquad (7)$$

In addition, secondary slip bands were often activated near the GB, as in the bicrystal B-200 (see Figs. 3b and 5). In this case, the effect of secondary slip bands on intergranular cracking should be taken into account. Fig. 8b schematically shows the interactions of slip bands with the GB in bicrystal B-200. Similar to Eq. (6), the Burgers vector sum b_{GB} of residual dislocations piled-up at the GB in bicrystal B-200 can be given as

$$b_{GB} = b_1 - b_2 - b_3 \qquad (8)$$

where, b_1, b_2 and b_3 are the Burgers vectors of residual dislocations carried by those slip bands in bicrystal B-200. According to the observations on surface slip morphology (see Figs. 3–5), it is apparent that the Burgers vector sum b_{GB} of residual dislocations piled-up at the GB in bicrystal B-200 will be not equal to 0, as in Eq. (7). In particular, those secondary slip bands may accelerate the formation of intergranular cracking for the bicrystal B-200. As those residual dislocations or vacancies piled-up at the GB are accumulated to a high density enough, intergranular fatigue cracking will occur along the GB under external stress. We can define this process as 'piling-up of defects'. It is consistent with the PSB-GB damage mechanism [10,19,22].

In previous reports [30–32], it was observed that fatigue cracking can take place along the slip bands rather than along GB or phase boundaries. Unfortunately, those observations of fatigue cracks were made by optical microscopy. Therefore, the true interface damage in those bicrystals after cyclic deformation cannot be clearly detected. Indeed, for the present bicrystals, GB cracking cannot be distinguished by optical microscopy, as shown in Fig. 3. But the SEM clearly revealed the intergranular fatigue cracking process of the bicrystals. Essentially, the accumulation of dislocations and vacancies at GB should be responsible for the intergranular cracking. It will explain why the GB is always stronger than the component crystals during tensile deformation of a ductile bicrystal. In this case, the deformation is unidirectional and the dislocations and vacancies piled-up at GB cannot be accumulated to high enough in density. Consequently, it can be concluded that the essence of intergranular fatigue cracking should be attributed to the reversal interactions of PSBs with GB, or the accumulation of dislocations and vacancies at GB. In other words, the PSB-GB mechanism will dominate the intergranular fatigue cracking of the present bicrystals. On the other hand, if it is considered that the steps cannot only be produced on the specimen surface along GB, but also in the interior of the GB plane by the interaction of PSB with GB. Those steps in the interior of the GB plane will be linked with further cyclic deformation and lead to GB crack nucleation and propagation for the bicrystal with a GB parallel to the stress axis. Then, the step-mechanism for intergranular fatigue cracking proposed by Kim and Laird [23,24] can also be used to explain the GB cracking of the present bicrystal. In combination with the intergranular cracking of those copper bicrystals with a perpendicular GB [25–29], it is suggested that the interaction of PSBs with the GB must be responsible for GB cracking no matter whether the GB was parallel, perpendicular or inclined to the stress axis in a bicrystal.

5. Conclusions

Based on the experimental results above, the following conclusions can be drawn

1. The saturation stresses of a $[\bar{4}\ 9\ 16]/[\bar{4}\ 9\ 27]$ copper bicrystal with a GB parallel to the stress axis increased with increasing strain amplitude. In particular, its saturation resolved shear stresses were obviously higher than the plateau stress of 28–30 MPa in copper single crystals oriented for single slip, if modified by an orientation factor of the bicrystal. Accordingly, a GB strengthening model was introduced. The increase in saturation stress of the bicrystals should be attributed to the GB resistance to PSBs or the strengthening effect of the GBAZ.
2. There existed serious plastic strain incompatibility near the GB, and a GBAZ with secondary slip formed in the bicrystals during cyclic deformation. Meanwhile, the GBAZ displayed some difference in width, total number of activated slip systems and the degree of plastic strain incompatibility. It is suggested that the total number of activated slip systems near a GB can be affected by the orientations of component crystals and the applied strain amplitude.

3. With further cyclic deformation, all the fatigue cracks nucleated and propagated along the GB in bicrystals B-50 and B-200. However, there was no crack nucleating along PSBs. It is indicated that intergranular fatigue cracking is the dominant damage mode even though the GB was parallel to the stress axis. By the interaction of PSBs with GB, an intergranular fatigue cracking mechanism produced by dislocation piling-up was introduced to the present copper bicrystal. It is concluded that the dislocation piling-up caused by the interactions of PSBs with GB should be responsible to intergranular fatigue cracking no matter whether the GB was parallel or perpendicular stress axis.

Acknowledgements

References

[1] H. Mughrabi, Mater. Sci. Eng. 33 (1978) 207.
[2] Z.S. Basinski, S.J. Basinski, Prog. Mater. Sci. 36 (1992) 89.
[3] A.S. Cheng, C. Laird, Mater. Sci. Eng. 51 (1981) 111.
[4] S.P. Bhat, C. Laird, Scr. Metall. 12 (1978) 687.
[5] K.V. Rasmussen, O.B. Pedersen, Acta Metall. 28 (1980) 1467.
[6] O.B. Pedersen, K.V. Rasmussen, Acta Metall. 30 (1982) 57.
[7] V.-J. Kuokkala, T. Lepisto, P. Kettunen, Scr. Metall. 16 (1982) 1149.
[8] H. Mughrabi, Scr. Metall. 13 (1979) 479.
[9] P. Lukas, L. Kunz, Mater. Sci. Eng. 74 (1985) L1.
[10] U. Essmann, U. Gosele, H. Mughrabi, Phil. Mag. A44 (1981) 405.
[11] A.S. Cheng, C. Laird, Fatigue Fract. Mater. Struct. 4 (1981) 331.
[12] Z.S. Basinski, S.J. Basinski, Acta Metall. 33 (1985) 1319.
[13] A. Hunshe, P. Neumann, Acta Metall. 34 (1986) 207.
[14] B.T. Ma, C. Laird, Acta Metall. 37 (1989) 325.
[15] E.A. Repetto, M. Ortiz, Acta Mater. 45 (1997) 2577.
[16] G.-H. Him, I.-B. Kwon, Mater. Sci. Eng. A142 (1991) 177.
[17] L.C. Lim, Acta Metall. 35 (1987) 1653.
[18] P. Gopalin, H. Margolin, Mater. Sci. Eng. A142 (1991) 11.
[19] W. Liu, M. Bayerlein, H. Mughrabi, A. Day, P.N. Queated, Acta Metall. Mater. 40 (1992) 1763.
[20] M.H. Yoo, A.H. King, Metall. Trans. 21A (1990) P2431.
[21] J. Polak, A. Vasek, K. Obrtlik, Fatigue Fract. Eng. Mater. Struct. 19 (1996) 147.
[22] H.-J. Christ, Mater. Sci. Eng. A117 (1989) 25.
[23] W.H. Kim, C. Laird, Acta Metall. 26 (1978) 777.
[24] W.H. Kim, C. Laird, Acta Metall. 26 (1978) 789.
[25] P. Peralta, C. Laird, Acta Mater. 45 (1997) 3029.
[26] Y.M. Hu, Z.G. Wang, Scr. Mater. 35 (1996) 1019.
[27] Y.M. Hu, Z.G. Wang, Int. J. Fatigue 19 (1997) 59.
[28] Y.M. Hu, Z.G. Wang, Int. J. Fatigue 20 (1998) 463.
[29] Z.F. Zhang, Z.G. Wang, Y.M. Hu, Mater. Sci. Eng. A 269 (1999) 136.
[30] H.D. Williams, G.C. Smith, Phil. Mag. 13 (1966) 835.
[31] J.C. Swearergen, R. Taggart, Acta Metall. 19 (1971) 543.
[32] H. Kawazoe, T. Takasugi, O. Izumi, Acta Metall. 28 (1980) 1253.
[33] Y.M. Hu, Z.G. Wang, G.Y. Li, Mater. Sci. Eng. A208 (1996) 260.
[34] Z.F. Zhang, Z.G. Wang, Acta Mater. 46 (1998) 5063.
[35] U.F. Kocks, Phil. Mag. 9A (1964) 187.
[36] C. Rey, A. Zaoui, Acta. Metall. 28 (1980) 687.
[37] C. Rey, A. Zaoui, Acta Metall. 30 (1982) 523.
[38] Y.-D. Chuang, H. Margolin, Metall.Trans. 4A (1973) 1905.
[39] T.-D. Lee, H. Margolin, Metall. Trans. 8A (1977) 145.
[40] T.-D. Lee, H. Margolin, Metall. Trans. 8A (1977) 157.